Journal of Geophysical Research: Biogeosciences

RESEARCH ARTICLE
10.1029/2018JG004494

Key Points:
- We found significant surface temperature differences over drained agricultural peatland and restored wetlands
- Restored wetlands' tall, emergent canopy structure delays heat exchange with the atmosphere, causing a daytime and growing season cooling effect
- Land use policy must consider biophysical impacts in addition to biogeochemical benefits, especially in novel land use transitions

Supporting Information:
- Supporting Information S1

Correspondence to:
K. S. Hemes,
khemes@berkeley.edu

Citation:
Hemes, K. S., Eichelmann, E., Chamberlain, S. D., Knox, S. H., Oikawa, P. Y., Sturtevant, C., et al. (2018). A unique combination of aerodynamic and surface properties contribute to surface cooling in restored wetlands of the Sacramento-San Joaquin Delta, California. *Journal of Geophysical Research: Biogeosciences*, *123*, 2072–2090. https://doi.org/10.1029/2018JG004494

Received 16 MAR 2018
Accepted 29 MAY 2018
Accepted article online 11 JUN 2018
Published online 10 JUL 2018

A Unique Combination of Aerodynamic and Surface Properties Contribute to Surface Cooling in Restored Wetlands of the Sacramento-San Joaquin Delta, California

Kyle S. Hemes[1], Elke Eichelmann[1], Samuel D. Chamberlain[1], Sara H. Knox[2], Patricia Y. Oikawa[3], Cove Sturtevant[4], Joseph Verfaillie[1], Daphne Szutu[1], and Dennis D. Baldocchi[1]

[1]Ecosystem Science Division, Department of Environmental Science, Policy and Management, University of California, Berkeley, CA, USA, [2]Department of Earth System Science, Stanford University, Stanford, CA, USA, [3]California State University, East Bay, Hayward, CA, USA, [4]National Ecological Observatory Network, Battelle Ecology, Boulder, CO, USA

Abstract Land use change and management affect climate by altering both the biogeochemical and biophysical interactions between the land and atmosphere. Whereas climate policy often emphasizes the biogeochemical impact of land use change, biophysical impacts, including changes in reflectance, energy partitioning among sensible and latent heat exchange, and surface roughness, can attenuate or enhance biogeochemical effects at local to regional scales. This study analyzes 3 years (2015–2017) of turbulent flux and meteorological data across three contrasting wetland restoration sites and one agricultural site, colocated in the Sacramento-San Joaquin Delta, California, USA, to understand if the biophysical impacts of freshwater wetland restoration can be expected to attenuate or enhance the potential biogeochemical benefits. We show that despite absorbing more net radiation, restored wetlands have the potential to cool daytime surface temperature by up to 5.1 °C, as compared to a dominant drained agricultural land use. Wetland canopy structure largely determines the magnitude of surface temperature cooling, with wetlands that contain areas of open water leading to enhanced nighttime latent heat flux and reduced diurnal temperate range. Daytime surface cooling could be important in ameliorating physiological stress associated with hotter and drier conditions and could also promote boundary layer feedbacks at the local to regional scale. With a renewed focus on the mitigation and adaptation potential of natural and working lands, we must better understand the role of biophysical changes, especially in novel land use transitions like wetland restoration.

Plain Language Summary Land use change and management affect climate by altering both the cycling of greenhouse gases and how energy and water are exchanged between the ecosystem and the atmosphere. These energy and water impacts can have local to regional implications on surface and air temperature. This study analyzes 3 years (2015–2017) of measured water and energy exchange at three contrasting wetland restoration sites and one agricultural site, all located in the Sacramento-San Joaquin Delta, California, USA. Restoring drained agricultural fields to flooded wetlands causes a rougher canopy, with more exposed water, and alters the energy partitioning. This results in growing season and daytime surface cooling, which could enhance the other benefits of wetland restoration, like soil buildup, habitat creation, and carbon sequestration. Land use policies should consider both the greenhouse gas and the energy and water implications of the promoted land use change to fully account for the climatic impact.

1. Introduction

Land use change and management affect climate by altering both the biogeochemical and biophysical processes that govern the exchange of greenhouse gases (GHG) and energy between the land and atmosphere (Anderson et al., 2011; Bonan, 2008; Luyssaert et al., 2014). Biogeochemical impacts are caused by changes in GHG exchange rates between ecosystems and the atmosphere, with net atmospheric increases in GHG concentrations resulting in increased radiative forcing (Arneth et al., 2010; Tian et al., 2016). Biophysical impacts of land use change include changes in reflectance, the partitioning of energy into latent and sensible heat exchange, surface roughness, and ultimately surface and mixed layer air temperature. These factors can attenuate or enhance biogeochemical effects at local to regional scales (Anderson et al., 2011; Bright et al., 2017; Jackson et al., 2008; Mahmood et al., 2014; Perugini et al., 2017; Rotenberg & Yakir, 2010; Zhao & Jackson, 2014).

Whereas much of the literature focuses exclusively on the biogeochemical impact of land use change (Mcalpine et al., 2010), the emphasis on biophysical impacts has been primarily limited to reforestation and deforestation scenarios (Alkama & Cescatti, 2016; Bonan, 2008; Burakowski et al., 2017; Juang et al., 2007; Lee et al., 2011; Lejeune et al., 2018; Perugini et al., 2017; Rotenberg & Yakir, 2010; Zhao & Jackson, 2014), woody vegetation encroachment (D'Odorico et al., 2010; He et al., 2015), and cropland management (Bonfils et al., 2007; Georgescu et al., 2011; Lobell et al., 2006; Lobell & Bonfils, 2008). With nascent policy mechanisms set to compensate landowners and farmers for low-emission land use practices, it is essential that they take into consideration how the biophysical impacts of novel land use changes could drive local- to regional-scale climatic perturbations, enhancing or attenuating the biogeochemical impacts. Beyond reforestation, few studies have explored the biophysical impacts of important types of land use change that have been proposed for climate change mitigation, such as restoring wetlands (Griscom et al., 2017; Paustian et al., 2016).

While flooded wetland systems have the potential to sequester carbon as photosynthesis outpaces oxygen-inhibited respiration, the highly reduced conditions can result in significant methane emissions (Bridgham et al., 2013; Dean et al., 2018; Petrescu et al., 2015). Restoring freshwater marshes has the potential to sequester significant amounts of carbon in accreted soil, as evidenced by the deep peatlands that have formed over thousands of years (Drexler et al., 2009), but come at the cost of significant methane emissions (Hatala et al., 2012; Hemes et al., 2018; Knox et al., 2015). The biophysical changes inherent in the transition from drained peatland agriculture to restored wetland, however, are not well established.

The Sacramento-San Joaquin Delta (hereafter, "Delta") provides an ideal system to understand the coupled biogeochemical and biophysical impacts of wetland restoration. The Delta has been subsiding dramatically since the midnineteenth century, in large part due to agricultural conversion of the natural freshwater wetlands (Weir, 1950). As the carbon-rich peat soil was drained and tilled, levees were erected to protect the "islands" from seasonal inundation. These processes exposed the previously flooded soil to oxygen and catalyzed aerobic oxidation, in some places leading to soil losses of up to 8 m (Deverel et al., 2016; Drexler et al., 2009). Efforts to rewet the peat soils through wetland restoration are attractive as climate mitigation activities, as well as to restore habitat and decrease hydrostatic pressure on levees that make up the Delta's fragile system of islands (Mount & Twiss, 2005). Measurements over a mesonetwork of restored wetlands in the Delta have shown that conversion of drained peatlands to wetlands can, in some cases, yield a net GHG benefit when compared to the original land use (Knox et al., 2015). Few studies have attempted to quantify the biophysical impacts of freshwater wetland restoration over such a network.

Part of the challenge in quantifying biophysical impacts of land use change stems from the fact that they consist of radiative (albedo) and nonradiative (evaporative efficiency and roughness) terms, often opposing in sign, that integrate to a net biophysical climatic impact (Bonan, 2008; Bright et al., 2017). Modification to the surface albedo changes the ratio of reflected to absorbed radiation, affecting the net radiation balance of the surface (Brovkin et al., 1999). The Intergovernmental Panel on Climate Change (IPCC) has included a term for radiative forcing associated with albedo changes due to anthropogenic land use and land cover change, which partially offsets the net positive radiative forcing associated with anthropogenic changes in the atmosphere (Myhre et al., 2013). Changes in surface properties also affect surface temperature and emissivity, which govern the longwave emissions from the surface.

Evaporative efficiency, or the partitioning of available energy into latent and sensible heat fluxes, can affect near-surface temperature and planetary boundary layer processes (Davin & de Noblet-Ducoudre, 2010; Luyssaert et al., 2014). Water availability at the surface of an ecosystem, which can be expressed through bulk surface conductance, largely determines whether available energy is partitioned into latent or sensible heat. Surface roughness, which controls the transfer of energy, mass, and momentum between the canopy and atmosphere, plays an important role in transferring this sensible and latent heat away from the surface, into the atmosphere (Verma, 1989). Enhanced surface roughness will increase the degree to which a canopy is coupled to the atmosphere (Jarvis & McNaughton, 1986) and affect turbulent fluxes. In turn, this can cause a surface temperature effect determined by the evaporative efficiency. Due to large uncertainties around the signs and magnitudes of the integrated biophysical impacts to climate, and the fact that a simple metric does not exist to reconcile radiative and nonradiative impacts on a global scale, the IPCC has omitted these nonradiative effects of land use change (Myhre et al., 2013).

Studies of biophysical impacts of land use change have been largely focused on transitions from field to forest, where competing effects of ecophysiological aerodynamics and albedo have been found to drive cooling (Juang et al., 2007). In a Mediterranean system, the potential air temperature over a rougher and less reflective oak woodland savannah was warmer than an aerodynamically smoother annual grassland (Baldocchi & Ma, 2013). Other work points to a latitudinal dependence on the temperature difference between open land and forested measurement sites (Davin & de Noblet-Ducoudre, 2010; Lee et al., 2011). Compared to open lands, forests tend to reduce the diurnal temperature range by cooling during the day (Lejeune et al., 2018) and warming at night (Lee et al., 2011), largely owing to roughness differences (Burakowski et al., 2017). Land use management associated with croplands has also been investigated at regional scales to understand near-surface temperature impacts associated with irrigation (Bonfils et al., 2007), tilling, and crop productivity (Lobell et al., 2006). Other important ecosystems beyond forests and irrigated croplands, like restored wetlands, have relatively few observations of biophysical climatic impacts.

This study analyzes 3 years (2015–2017) of eddy covariance flux and meteorological data across three wetland restoration sites and one drained peatland agriculture site colocated in the Delta. The restored wetland sites, all constructed with managed water tables, differ somewhat in their species mix, areal extent, bathymetry, and years since restoration but are all subject to similar meteorological drivers due to their close spatial proximity ($<$13 km). Using eddy covariance and associated meteorological and environmental measurements, we test the hypothesis that restored wetlands will have a cooling effect on surface temperature.

We expect low-albedo wetland surfaces to take up more net radiation, which will be stored in the water column, or preferentially partitioned into latent heat flux, increasing evaporative efficiency. The wetlands' aerodynamically rougher canopy structure will enhance turbulent mixing of heat fluxes away from the canopy. We propose that wetland restoration, in the transition from an aerodynamically smooth and short-statured agricultural crop to dense, emergent wetland species, may mimic some of the biophysical surface dynamics that characterize reforestation. Computations of aerodynamic surface temperature and energy balance differences, along with an assessment of canopy conductance properties, will allow us to diagnose the biophysical differences between a drained agricultural peatland and the various restored wetlands. This study aims to understand if the biophysical impacts of restoration at the local scale can be expected to attenuate or enhance the potential biogeochemical benefits of freshwater wetland restoration. It also aims to understand the potential implications of regional-scale wetland restoration on plant physiology and mixed layer air temperature.

2. Data and Methods

2.1. Site Characteristics

The Sacramento-San Joaquin Delta lies at the confluence of two of California's major rivers and formed a historic 1,400 km^2 freshwater wetland landscape at near-sea level (Atwater et al., 1979). In the midnineteenth century, the wetland was diked and drained for agricultural purposes, exposing deep peat soils to oxygen. Today, more than 1,700 km of dikes and levees hold back the rivers and sloughs that make up the modern Delta (Mount & Twiss, 2005). The Delta is critical to California's water storage and transport system; the rivers that feed the Delta provide at least a portion of the drinking water to more than two thirds of Californians through the State Water Project and the Central Valley Project (Miller et al., 2008). The Delta's wetland soils are highly organic, while the agricultural soils exhibit a degraded, oxidized peat surface layer underlain by a deep peat horizon (Miller et al., 2008). The remaining peat is estimated to be 4,000–6,000 years old (Drexler et al., 2009; Weir, 1950).

To understand the biophysical impacts of land use change, the three restored wetland sites, designated young wetland, intermediate wetland, and old wetland (which refers to their age since restoration), are each compared to alfalfa, a drained agricultural peatland land use. While the Delta has supported a number of agricultural crops since drainage and "reclamation" in the midnineteenth century, alfalfa (*Medicago sativa* L.) shares a perennial life cycle strategy with the dominant tule (*Schoenoplectus acutus*) and cattail (*Typha* spp.) wetland species and represents one of the most important agricultural crops in the five-county Delta region and California as a whole. In 2015, more than 80,000 acres were planted with alfalfa in the Delta region, representing 11.8% of the region's land cover (Medellín-Azuara et al., 2016). All sites have been described in previous studies and will be summarized here for brevity (Eichelmann et al., 2018; Knox et al., 2015).

Table 1
Site Characteristics

Land use type	Site (Ameriflux ID and DOI)	Land use history	Location	Albedo (min/max)	Measurement height/mean canopy height** (m)
alfalfa	Alfalfa (US-TW3; 10.17190/AMF/1246149)	30 ha Alfalfa since 2010, previously corn	Twitchell Island. 38.1159 N, −121.6467 W	0.142/0.248	2.9/0.4***
young wetland	East End (US-TW4; 10.17190/AMF/1246151)	323 ha wetland restored in 2013	Twitchell Island. 38.1030 N, −121.6414 W	0.097/0.142	4.9/2.2
intermediate wetland	Mayberry (US-MYB; 10.17190/AMF/1246139)	121 ha wetland restored in 2010	Sherman Island. 38.0498 N, −121.7651 W	0.122/0.134*	5.1/3.4
old wetland	West Pond (US-TW1; 10.17190/AMF/1246147)	3 ha wetland restored in 1997	Twitchell Island. 38.1074 N, −121.6469 W	0.108/0.142	4.5/2.6

Note. Maximum and minimum mean monthly midday shortwave albedo as measured with a tower-mounted four-way net radiometer (*intermediate wetland site albedo estimated from annual footprint averaged min/max values extracted from Moderate Resolution Imaging Spectroradiometer albedo product MCD43A; ** measurement height measured from water surface at wetland sites, mean canopy height computed from turbulent statistics; ***vegetation height varies from 0.1 to 0.6 cm depending on time since cutting).

The alfalfa (US-TW3, Twitchell Alfalfa) site is an alfalfa field on Twitchell Island, previously planted in corn (Baldocchi, 2018a). Alfalfa is subirrigated, harvested between five and seven times a year, beginning in mid-March, and is periodically grazed with sheep. Alfalfa is California's largest agricultural water user and is, like the wetland systems, a perennial with a long growing season (Hanson et al., 2007). While the full record of the alfalfa crop was preserved to represent the actual state of the agro-ecosystem, the periodic cuttings did affect the surface energy balance. Tests excluding the 5–10 days after cutting to remove this effect had minor impacts on the results.

The young wetland (US-TW4, East End) was constructed in late 2013 after being under continuous corn cultivation (Baldocchi, 2018b). Since initial flooding, the wetland filled in with tule and cattail vegetation and represents an early-intermediate stage of restoration, with limited patches of open water. The 90% average cumulative eddy covariance flux footprint spans 390 m in the west-southwest direction (Eichelmann et al., 2018). The early years of the young wetland's restoration exhibited very dynamic changes in vegetation structure and extent as vegetation filled in. Due to a faulty wiring connection, horizontal wind speed and direction data over a period between July 2015 and January 2016 were corrupted and are thus omitted from the young wetland record.

The intermediate restored wetland (US-MYB, Mayberry) was constructed in 2010 on Sherman Island (Baldocchi, 2018c). With a water table as deep as 2 m in open water channels, the intermediate wetland is the most heterogeneous of the three restored wetland treatments in this study. The 90% average cumulative eddy covariance flux footprint spans 350 m in the west-northwest direction capturing large areas of open water and patches of vegetation (Eichelmann et al., 2018). Additionally, rising salinity levels during drought years and insect infestation in the wetland caused lowered productivity throughout the study period. This wetland is also vegetated with a mixture of tule and cattail.

The old restored wetland (US-TW1, West Pond) was constructed in 1997 as the pilot restored wetland for the ongoing study on Twitchell Island (Baldocchi, 2018d). We began eddy flux measurements in summer 2012. The old wetland, which is dominated by tall, emergent tule and cattail, represents a mature restored wetland and has no open water patches. The 90% average cumulative eddy covariance flux footprint spans 260 m in the west-southwest direction (Eichelmann et al., 2018).

2.2. Eddy Covariance Measurements and Processing

2.2.1. Site Setup

We used the eddy covariance method (Baldocchi et al., 1988) to measure continuous fluxes of H_2O, CO_2, and sensible heat at all sites. Fluxes were measured at a frequency of 20 Hz, using open-path infrared gas analyzers (LI-7500 or LI-7500A, LiCOR Inc., Lincoln, NE, USA) that are calibrated every 3–6 months in the lab (LI-7500). Sonic anemometers measure sonic temperature and three-dimensional wind speeds at 20 Hz (WindMaster Pro 1352, Gill Instruments Ltd, Lymington, Hampshire, England). All instruments are mounted on towers at a height of 2.9 to 5.1 m above the surface (Table 1), in such an orientation as to prevent interference with winds from the dominant direction.

By most standards, the study sites provide near-ideal conditions for measuring turbulent fluxes using the eddy covariance method (Baldocchi et al., 1988). The study sites are exceedingly flat, have large fetches,

and exhibit brisk daytime and nighttime winds. Sampling is at sufficiently high resolution to capture most of the flux-containing eddies and to minimize filtering of the flux signal by the separation of the instruments and the path separation of the transducers. The instrument setup (sampling rate, sensor separation, fetch, and sensor height) was designed to optimize the measured cospectrum and minimize spectral filtering (Detto et al., 2010). Typical cospectra exhibit slopes that closely match the idealized slope from Kaimal et al. (1972). The main complication affecting the interpretation of our fluxes is the relative lack of homogeneity of the footprint of the restored wetlands, a mosaic of open water and vegetation.

Energy balance closure serves as a metric to evaluate scalar flux measurements when using the eddy covariance method over terrestrial ecosystems (Wilson et al., 2002). Ground heat flux (G) is not measured at the old or intermediate wetland sites but is expected to be small due to the water layer dampening the energy flux into the soil. Storage flux (S) in the water column of the wetlands is significant, due to the high heat capacity of water, especially in wetlands with open water surfaces. While multilevel temperature profiles are deployed at the towers, storage flux is challenging to accurately predict due to nonhorizontally isothermal conditions, complex bathymetry at the sites, and variable vegetation shading and insulation. In addition, water table height changes depending on pumping, evaporation, and precipitation. The available measurements represent limited sample areas compared to the integrated footprint of latent and sensible heat fluxes provided by the eddy covariance measurements.

For these reasons, half-hourly energy balance closure over the 3-year study period is best at the alfalfa and old wetland sites with closed canopies (79.3% and 78.1%, respectively). The young and intermediate wetlands, with large tracts of open water storing energy, are further from closure (55.8% and 65.2%, respectively), indicating the inability to measure the available energy terms (G and S) completely and representatively across the complex footprint (Eichelmann et al., 2018). To more adequately and consistently represent storage at all sites in our analysis, we use the residual of the energy balance to compute a combined soil and water storage term as

$$S_{\text{residual}} = \text{RNET} - \lambda E - H \quad \left(\text{W m}^{-2}\right)$$

where RNET is the net radiation as measured by the radiometer, λE is the latent heat flux, and H is the sensible heat flux, both measured by eddy covariance.

2.2.2. Processing and Gap Filling

Trace gas and energy fluxes were calculated using the 30-min covariance of turbulent fluctuations in vertical wind speed and scalar of interest after applying a series of standard corrections and site-specific factors (Detto et al., 2010; Hatala et al., 2012; Knox et al., 2015). Coordinate rotations were performed so that mean wind speeds at each 30-min averaging interval were zero in the cross-wind and vertical directions. To account for air density fluctuations, the Webb-Pearman-Leuning corrections were applied (Webb et al., 1980). To remove flux data measured over nonideal conditions, half-hourly fluxes were filtered for stability and turbulence, friction velocity, wind direction, spikes in mean densities, variances and covariances, and sensor window obstruction.

To integrate yearly budgets, we gap filled fluxes by training an Artificial Neural Network (ANN) using measured meteorological variables (Moffat et al., 2007; Papale et al., 2006). Training, validation, and testing data were selected from a series of k-means clusters to avoid seasonal or diurnal bias (Mathworks Inc., Natick, MA, USA). Network architecture with varying levels of complexity was tested, with the simplest architecture selected for which further increases in complexity yielded less than a 5% reduction in mean standard error (Knox et al., 2015, 2016). This entire ANN procedure was performed 20 times, producing 20 separate ANNs. The median prediction of the 20 ANNs was used to fill gaps in the annual data, with linear correlation fits of 94%, 91%, 88%, and 98% (alfalfa, young wetland, intermediate wetland, and old wetland, respectively) for λE flux and 96%, 96%, 93%, and 98% for H flux.

2.3. Temperature Measurements

Different temperature metrics can reveal various aspects of heat exchange between the landscape and the atmosphere. Near-surface air temperature is convenient for scaling observations with basic meteorological data but is influenced by measurement height, as well as local meteorological and atmospheric stability. Radiative temperature, derived from radiative longwave emission and knowledge of surface emissivity, can

reveal the temperature at the leaf. It can be biased if the canopy is open and the background surface temperature is much greater than the leaf temperature. Furthermore, the sampling area of the radiometer depends on its field of view, angle of observation, and height above the surface, making it often unrepresentative of large heterogeneous footprints. Aerodynamic temperature, derived from canopy aerodynamic properties and sensible heat flux, yields the temperature of the surface that drives turbulent fluxes. It represents a large footprint, samples sunlit and shaded leaves, and may be the most representative measure of the temperature that organisms experience at the landscape scale (Verma, 1989). For these reasons, we used aerodynamic surface temperature (T_{aero}) as our metric for the integrated biophysical impacts of land use change. Aerodynamic surface temperature is defined as

$$T_{aero} = \frac{H}{\rho C_p G_{aero}} + T_{air} \quad (°C)$$

where T_{air} is measured with aspirated and wind-shielded humidity and temperature probes (HMP-60, Vaisala Inc., Helsinki, Finland) colocated with the gas analyzers (accuracy ±0.5 °C). To remove intersite T_{air} calibration bias, T_{air} was corrected to a colocated, recently factory-calibrated sensor. H represents half-hourly sensible heat flux measurements, ρ is density of dry air, C_p is the specific heat of air at a constant pressure, and G_{aero} is the canopy aerodynamic conductance to heat exchange (as calculated below). Surface temperature differences, ΔT_{aero} (°C), are calculated as the half-hour temperature difference between sites, averaged over a month or a specific half hour of the day to assess seasonal and diel trends, respectively. As a measure of uncertainty, T_{aero} and energy flux differences are displayed with 95% confidence intervals.

To understand the importance of daytime T_{aero} changes, we used a nonparametric binning approach to extract a functional pattern (Falge et al., 2001; Ma et al., 2017). We sorted the flux data by temperature and then binned successive pairs of net ecosystem productivity (NEP) and concurrent T_{aero} with a fixed sample size (n = 50) per bin, to prevent skewness due to uneven numbers of samples per bin (J. G. Barr et al., 2013). Prior to binning, the data were filtered by light level (photosynthetically active radiation >1,500 μmol m^{-2}) to focus on high-radiation midday growth periods. Although we recognize that this analytical method includes confounding effects such as phenological stage, vapor pressure deficit, and variable species mix, it capitalizes on the large sample sizes inherent to continuous eddy covariance measurements to effectively produce a response function.

2.4. Aerodynamic and Surface Conductance

We diagnosed the biophysical controls on surface energy fluxes by evaluating the surface conductance from the Penman Monteith equation (Monteith, 1965). The Penman-Monteith equation describes evapotranspiration by reconciling the energy supply and stomatal demand for water and, at the canopy scale, acts as a weighted sum of the stomatal conductance of the measured flux footprint. By inverting the Penman-Monteith equation (Monteith, 1981), surface conductance can be derived as

$$G_{sfc} = \frac{(\gamma * G_{aero} * \lambda E)}{(s * A) + \rho * C_\rho * \mathrm{VPD} * G_{aero} - \lambda E * (s + \gamma)} \quad \left(\mathrm{m\ s^{-1}}\right)$$

where γ is the psychometric constant, s is the slope of saturation vapor pressure-temperature curve, VPD is the atmospheric vapor pressure deficit, and A is the available energy defined as

$$A = \lambda E + H \quad \left(\mathrm{W\ m^{-2}}\right)$$

Because S is challenging to measure across the heterogeneous bathymetry of a restored wetland's footprint, as explained above, λE and H were used to compute available energy in the inverted Penman-Monteith equation for all sites (Humphreys et al., 2006).

To account for the structural differences between land use types, we calculated the aerodynamic conductance, which, for an integrated canopy, is the inverse of the sum of the turbulent and laminar boundary layer resistance (Verma, 1989);

$$R_{aero} = R_{turbulent} + R_{boundary\ layer}$$

where

$$R_{\text{turbulent}} = \frac{\overline{u}}{ustar^2} \quad \left(\text{s m}^{-1}\right)$$

and

$$R_{\text{boundary layer}} = 6.2 * ustar^{-2/3} \quad \left(\text{s m}^{-1}\right)$$

and

$$G_{\text{aero}} = \frac{1}{R_{\text{aero}}} \quad \text{m s}^{-1}$$

where $\overline{u}$ is the average wind speed in the horizontal direction as measured by the tower-based sonic anemometer and ustar is the average friction velocity, a function of the Reynold's shear stress or average covariance between upward and horizontal instantaneous wind speeds, measured at the eddy covariance tower. Laminar boundary layer resistance ($R_{\text{boundary layer}}$) is modeled after Thom (1972); this empirical formulation has been shown to result in values sufficiently similar to a more complicated physically based approach (Knauer et al., 2017). Due to noise in the observed data, raw conductance is filtered by cutting outliers in the percentile below 1% and above 99%, followed by omitting spurious negative values. As a measure of uncertainty, seasonal and diel G_{sfc} are displayed with 95% confidence intervals.

Measurement height discrepancies between alfalfa (2.8 m) and wetland sites (~5 m) have minor effects on T_{air} and $\overline{u}$. We performed sensitivity tests on the measurement height of alfalfa by computing T_{aero} with modeled $\overline{u}$ at 5 m based on the log wind profile. T_{aero} at the measured (2.8 m) and modeled (5 m) heights differs by ~4% at the half-hourly scale and ~0.2% at the daily scale; a simple two-sample t test does not reject the null hypothesis that the measured and modeled T_{aero} have equal means. For these reasons, and to avoid unnecessary assumptions of the log wind profile, data presented here are from the measured 2.8-m measurement height at alfalfa.

2.5. Boundary Layer Feedbacks

To understand the implications of T_{aero} changes associated with different land use types studied, we employed a simple energy balance-planetary boundary layer (EB-PBL) model (Baldocchi & Ma, 2013). The model couples an analytical solution (Paw U & Gao, 1988) to the surface energy balance with a one-dimensional PBL growth model (A. G. Barr & Betts, 1997; McNaughton & Spriggs, 1986), considering a single column of air, and solves for moisture and heat fluxes into or out of the top and bottom. The model assumes infinite spatial homogeneity and returns surface and mixed layer air temperatures. It is run for a single clear-sky growing season day, with measured VPD and incoming radiation, where available. Initial boundary layer height is set at 100 m (Bianco et al., 2011). Surface characteristics are proscribed (Figure S5 in the supporting information) with G_{aero} and G_{sfc} computed from eddy covariance data, as presented in results below.

3. Results

3.1. Seasonal Patterns of Temperature, Energy Balance, and Surface Properties

To understand the impact of land use change on local microclimate, we compare T_{aero} and energy balance components of the restored wetland sites with the alfalfa site. Over a network of restored wetlands, we can address the question—what are the impacts of restoring a smooth statured, well-irrigated perennial crop with a darker, taller, and rougher managed wetland? By convention, the alfalfa land use is subtracted from each wetland land use, so that positive values indicate warmer temperatures or more heat flux at the wetland sites. Finally, we present G_{sfc} and G_{aero} dynamics to investigate how wetland structure impacts turbulent fluxes and ultimately, T_{aero}.

3.1.1. Seasonal Temperature and Energy Balance Differences

Monthly average wetland T_{aero} was cooler than alfalfa T_{aero} during the height of the growing season (Figure 1). During other times of the year, especially during the spring, the wetland's T_{aero} was warmer than alfalfa's, by up to 2.3°C (Table S1). To understand how the underlying turbulent heat fluxes drive this observed

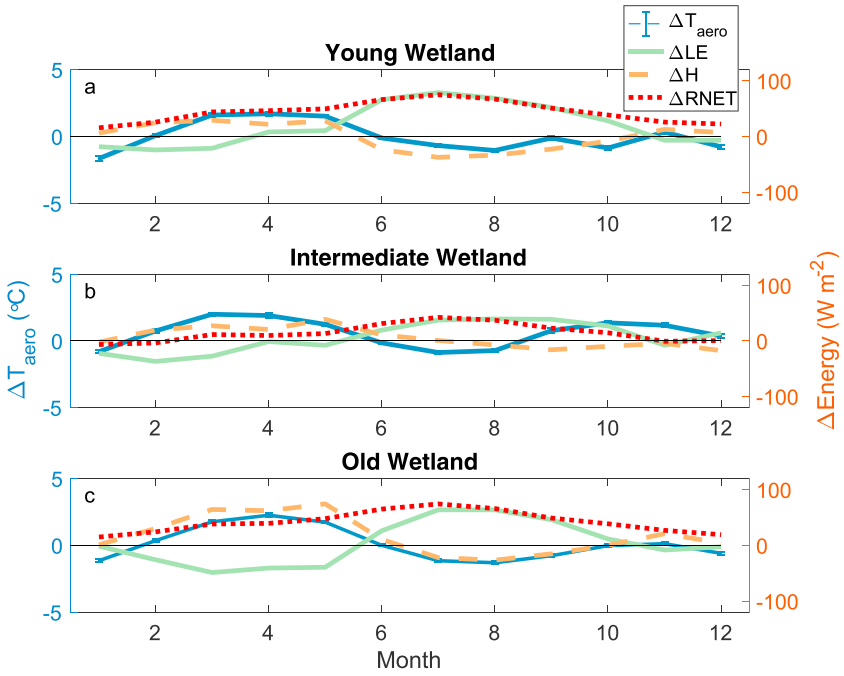

Figure 1. Average monthly aerodynamic temperature and energy flux differences between the (a) young wetland, (b) intermediate wetland, and (c) old wetland and the alfalfa site. Error bars on the aerodynamic temperature difference line represent 95% confidence intervals but are not easily distinguishable due to their small size.

seasonal T_{aero} difference, we take an energy balance approach. Each term of the energy balance equation is compared by taking the difference between the respective wetland and the alfalfa land use (Table S1).

The wetland sites receive more net radiation most months of the year, compared to alfalfa (Figure 1). Because incoming shortwave radiation is very comparable at all the sites due to proximity, net radiation differences are primarily a function of albedo and T_{aero}. Taller wetland vegetation is expected to have a lower albedo as it traps light more effectively than short, herbaceous vegetation (Cescatti et al., 2012; Stanhill, 1970). Additionally, the dark water surfaces at the restored wetland sites lower albedo to nearly half that at alfalfa (Table 1). An increase in net radiation at the wetland sites due to lowered albedo translates into increased available energy that can be partitioned into sensible heat, latent heat, and storage.

During June, July, and August, the young wetland's enhanced latent heat and diminished sensible heat compared to alfalfa are concurrent with nearly equivalent or cooler T_{aero} at the wetland (Figure 1a). At the intermediate wetland site, we see a similar pattern. Excess radiation taken up by the wetland is almost completely emitted as latent energy during the growing season. This is concurrent with T_{aero} up to 0.87 °C cooler than alfalfa (Figure 1b). The old wetland exhibits significantly more sensible heat flux and less latent heat flux than alfalfa until early summer, when latent heat flux begins to outpace that at alfalfa (Figure 1c). Surface temperatures at the old wetland become cooler than those at alfalfa when the wetland latent energy enhancement is maximized, in July and August.

3.1.2. Seasonal Aerodynamic and Surface Properties

To further diagnose the mechanisms driving the observed temperature and energy balance discrepancies, we assessed the aerodynamic and surface properties of the land use types. Average seasonal cycles of G_{aero} and G_{sfc} reveal characteristic differences in the land uses that impact how energy and matter are exchanged with the atmosphere. At all sites, G_{aero} is considerably larger than the G_{sfc} (Figure 2a, note the scales of axes), indicating the importance of canopy structure and roughness on turbulent exchange, especially in the windy environment of the Sacramento-San Joaquin Delta.

Peak G_{aero} at the old (0.041 m s^{-1}), intermediate (0.044 m s^{-1}), and young wetland (0.037 m s^{-1}) sites are nearly double the magnitude of the peak G_{aero} at the short-statured and relatively smooth alfalfa site

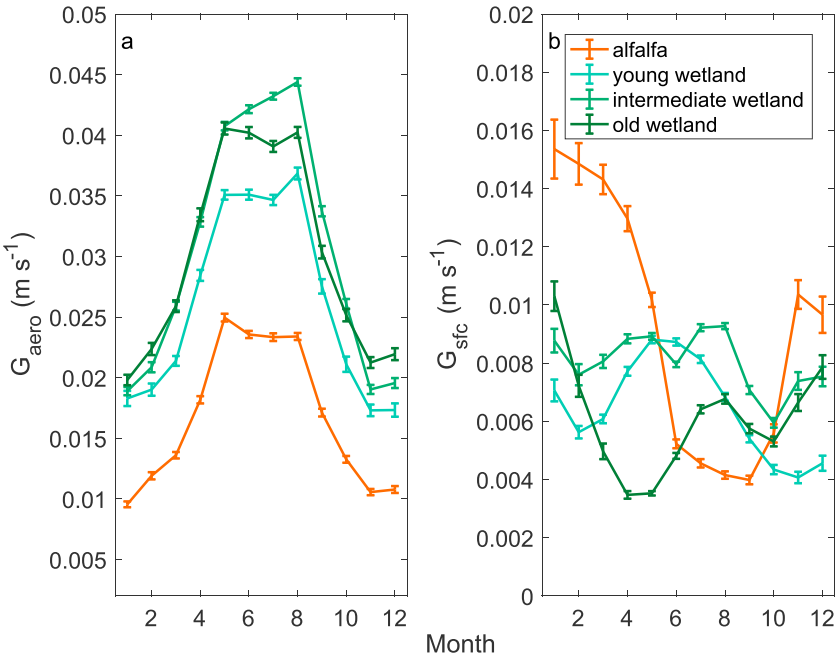

Figure 2. Mean monthly (a) aerodynamic and (b) surface conductance at each of the four study sites (m s^{-1}). Error bars represent 95% confidence intervals of the conductance.

(0.025 m s^{-1}; Figure 2a). At all sites, the seasonal cycle of G_{aero} is similar. Alfalfa peaks early, in May, while the wetland crops peak toward the end of the summer growing season, when the wetlands are fully emergent with tule and cattail species extending 2–3 m from the water level. Winter G_{aero} of senescent vegetation hovers below 0.02 m/s at the wetland sites. Alfalfa's winter G_{aero} drops to less than half that (Figure 2a).

While G_{aero} reveals the impact of turbulent mixing conditions promoted by the canopy structure, G_{sfc} tells us about the availability of water both through transpiration and evaporation (Jarvis & McNaughton, 1986; Raupach, 1998). Seasonal G_{sfc} patterns exhibit markedly different dynamics among sites (Figure 2b). Alfalfa's G_{sfc} peaks early in the year (0.015 m/s) and falls off throughout the main growing season to a minimum in September (0.004 m/s), recovering when the cooler, wetter conditions of the winter return. Wet winter months, in which the perennial crop cover is spotty but the soil retains moisture, are likely contributing to the midwinter maxima. The growing season decline is driven by high temperatures and uncertain access to ground water at the site throughout the summer (Figure S1). The older wetland's G_{sfc} exhibits a spring minimum, with maximum G_{sfc} values in the winter months (0.01 m/s), and a secondary peak during green-up in midsummer.

The young wetland, with decreasing contributions from open water throughout the study period, exhibits maximum G_{sfc} (0.009 m/s) during May growth, with a gradual decline over the summer months. The intermediate wetland sustains a high G_{sfc} throughout the growing season, falling off as the plants senesce in late summer. As G_{sfc} represents an integrated footprint conductance value, the heterogeneous nature of these younger wetlands means that G_{sfc} is a combination of transpiration through stomata and evaporation through open water surfaces, which have very different mechanistic controls (Goulden et al., 2007).

Direct comparisons of the magnitudes of G_{sfc} between the alfalfa and the respective wetland sites show a seasonal bias toward higher values, especially at the more heterogenous young and intermediate wetlands (Figures S2a and S2b). This contrasts with G_{aero}, which exhibits an annual bias toward significantly higher values at all of the wetland sites, with the largest magnitudes during the growing season (Figures S2d–S2f). In general, the land use transition from drained alfalfa to flooded wetland is characterized by an increased growing season G_{sfc} and an increased year-round G_{aero}.

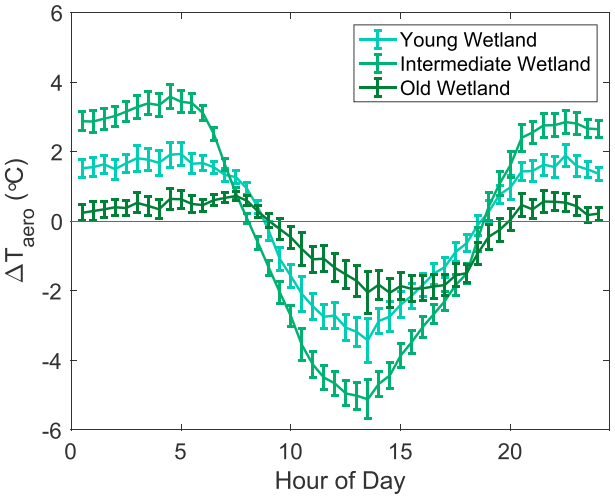

Figure 3. Average diel aerodynamic temperature differences between the respective wetland sites and alfalfa during the growing season (May–September). Error bars represent 95% confidence intervals of the half-hourly mean growing season temperature difference.

3.2. Diel Patterns of Temperature, Energy Balance, and Surface Properties

Mean monthly values are useful for understanding long-term seasonal trends but can mask important diel differences driven primarily by daily cycles of radiation. Here we present patterns of T_{aero}, energy balance components, and G_{sfc} and G_{aero} at the diel scale, focusing on the growing season (May–September).

3.2.1. Diel Temperature and Energy Balance Differences

Diel T_{aero} differences between the wetland sites and the alfalfa site vary considerably depending on the wetland structure. Each of the wetlands was significantly cooler than the alfalfa site during the day and warmer than the alfalfa site during the night. The young wetland was up to 3.4 °C (occurring at 13:30) cooler than alfalfa during the daytime and up to 1.9 °C warmer throughout the night. Similarly, the intermediate wetland was up to 5.1 °C (13:30) cooler than alfalfa during the daytime and up to 3.6 °C warmer during the night. The old wetland displays a similar but more dampened diel cycle of temperature difference, with slightly cooler temperatures of up to 2.1 °C (14:30) during the day and warmer temperatures of up to 0.7 °C during the night (Figure 3). These differences suggest that the way incoming solar radiation is partitioned into turbulent heat fluxes at each of the sites affects the magnitude of the daytime cooling effect at the wetland sites.

Diel patterns of sensible and latent energy flux differences between the site pairs emphasize the importance of wetland canopy structure on biophysical properties (Figures 4c, 4d, and S3). These structural characteristics include height, roughness, fraction of live and dead biomass, and the ratio of vegetation to open water. Owing to the decreased albedo of the dark vegetation and water surfaces, and increased leaf area index that

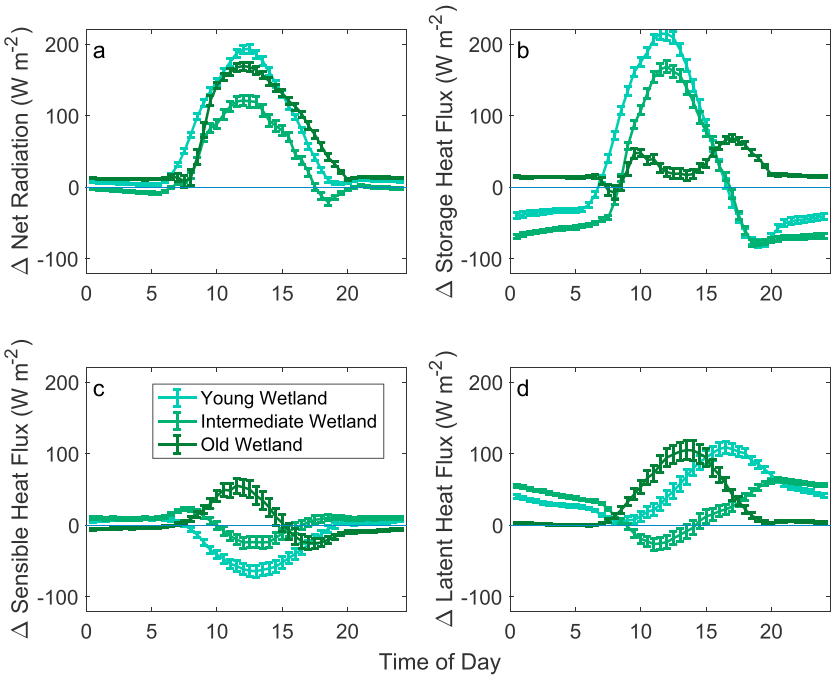

Figure 4. Diel growing season differences in (a) net radiation, (b) residual storage flux, (c) sensible heat flux, and (d) latent heat flux between the respective wetland sites and alfalfa. Error bars represent 95% confidence intervals of the half-hourly mean growing season energy fluxes.

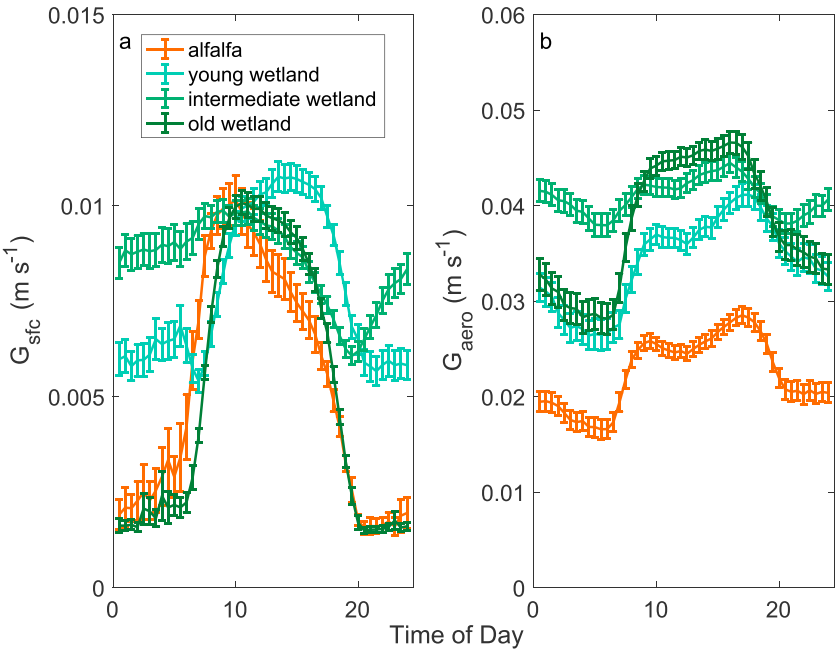

Figure 5. Diel growing season surface and aerodynamic conductance at each site (m/s^1) (note that the scale of the *y* axes differ). Error bars represent 95% confidence intervals of the half-hourly mean growing season conductance.

can effectively trap photons, net radiation during the growing season was much larger at the wetland sites than at alfalfa (Figure 4a).

The young wetland receives up to 193 W m^{-2} of additional daytime net radiation as compared to alfalfa during the growing season (Figure 4a). Much of this excess radiation is stored in the water column during the day, considerably more daytime storage than at alfalfa or the old wetland (Figure 4b). This storage results in cooler T_{aero} and thus diminished sensible heat flux during the day compared to alfalfa, as less energy is available for partitioning into turbulent fluxes (Figure 4c). The daytime T_{aero} cooling effect at the wetlands with open water surfaces (Figure 3) is concurrent with a reduction in daytime sensible heat flux. Importantly, it also results in a release of the energy stored in the water as latent heat flux during the night (Figure 4d). The intermediate wetland exhibited similar patterns to the young wetland, with enhanced daytime storage flux and nighttime latent heat flux compared to the alfalfa site.

The old wetland exhibited a different diel pattern of growing season energy balance differences. Much less of the old wetland's excess radiation was stored in the water column (Figure 4b). Instead of diminished daytime turbulent heat fluxes, as in the other wetlands, the old wetland's increased net radiation (Figure 4a) and high G_{aero} (Figure 5b) drove enhanced daytime sensible and latent heat flux. This enhanced daytime sensible and latent heat flux heat removed heat from the surface, but less effectively than through water column storage, evidenced by less of a daytime cooling effect at the old wetland (Figure 3). Nighttime turbulent heat fluxes were near zero at both the old wetland and alfalfa (Figures 4c and 4d), and storage heat flux showed little difference between the old wetland and the alfalfa site (Figure 4b).

3.2.2. Diel Aerodynamic and Surface Properties

Average growing season diel trends reveal the reliance of G_{sfc} on stomatal dynamics. Both alfalfa and the old wetland, with homogenous canopy cover and little open soil or water, had a distinct diel cycle of high G_{sfc} during active photosynthesis in the daytime (0.011 and 0.010 m/s, respectively) and near zero G_{sfc} at night (0.002 m/s) (Figure 5a). Both sites' diel cycles peaked around late morning and dropped off throughout the day, likely a response to high growing season T_{air} and vapor pressure deficit (VPD). While high VPD and T_{air} would promote evaporation even after stomata close, a lack of open water surfaces result in dramatically declining G_{sfc} during the afternoon and night. This is in contrast to the young and intermediate wetlands, which exhibit heightened G_{sfc} throughout the diel period (Figure 5a). While the intermediate wetland's G_{sfc}

is reduced during the afternoon, likely due to stomatal closure on hot, dry growing season days, its G_{sfc} appears to recover overnight. Nighttime stomatal conductance was confirmed to be near zero in a leaf-level measurement campaign (data not shown), indicating that heightened nighttime G_{sfc} is largely a result of evaporation from the open water surfaces characteristic of the young and intermediate wetlands.

Diel growing season G_{aero} at the wetland sites was close to 2 times those at the smooth, short-statured alfalfa site, reaching up to 0.047 m/s^1 at the old wetland (Figure 5b). G_{aero} maxima follow the age of the wetland, suggesting that the more mature, taller structure promotes high G_{aero} values. All sites follow a similar diel cycle, characterized by a daytime plateau.

4. Discussion

4.1. Biophysical Differences Between Sites

Drained peatland agriculture is the dominant land use in the Delta region, and nascent policy mechanisms are aiming to incentivize restoration to an ecosystem resembling the preindustrial inland freshwater wetlands. These policy mechanisms primarily focus on the biogeochemical benefit of the land use change. Here we explore the biophysical impacts of wetland restoration- how this land use transition changes the surface properties to have an integrated impact on T_{aero}. Despite similar meteorological conditions, significant T_{aero} differences emerged both seasonally (Figure 1) and diurnally (Figure 3) across the study sites due to the way that the ecosystems differentially exchange energy and momentum with the atmosphere.

At the seasonal scale, wetland T_{aero} was up to 2.3 °C warmer than alfalfa (Figure 1), mostly during the spring and autumn. High leaf area index and dark water surfaces at the wetland sites absorbed much more net radiation than the alfalfa land cover. During growing season periods, enhanced G_{sfc} and G_{aero}, along with higher latent heat flux at the wetland sites, drove monthly mean T_{aero} lower than those at alfalfa. These results contrast with T_{aero} dynamics from thaw-induced boreal wetland expansion, where a wetland cooling effect was observed to be maximum during late winter and moderate in summer (Helbig et al., 2016). In that case, however, aerodynamically rough jack pine stands were being compared to relatively short-statured wetland ecosystems. Seasonal patterns alone are not sufficient to understand how biophysical properties affect T_{aero}, as they mask important diel variations driven by radiation.

On an average growing season day, during midday, the young, intermediate, and old wetlands cooled the surface by up to 3.4 °C, 5.1 °C, and 2.1 °C, respectively (Figure 3). Diel temperature differences revealed that in addition to the land cover transition itself, the structure of the restored wetland determined the magnitude of the T_{aero} effect. The young and intermediate wetlands, with patches of open water interspersed between vegetation, provided more daytime cooling than the old wetland, with a mature, dense, closed canopy cover. Conversely, the open water wetlands were warmer during the night (Figure 3). By analyzing the differences in each energy balance term between the various wetlands and alfalfa, alongside the patterns of G_{sfc} and G_{aero}, we can understand the drivers of the observed seasonal and diel T_{aero} differences.

The young and intermediate wetlands store much of their enhanced net radiation during the day within the water column (Figure 4b). This storage reduces the latent and sensible heat flux during the day, temporarily decoupling the incoming radiation from the outgoing heat fluxes. This temporal decoupling results in a cooling effect of the T_{aero} during the day, compared to alfalfa (Figure 3). Beginning in the early evening and throughout the night, much of this stored energy is released. With high G_{aero} due to the tall, emergent properties of the wetland species (Figure 5b) and heightened G_{sfc} despite closed stomata due to the surfaces of open water (Figure 5a), much of this nighttime heat flux is released in the form of latent energy, humidifying the low, stable boundary layer and contributing to enhanced nighttime T_{aero} compared to alfalfa (Figure 3).

Aerodynamic conductance represents how well latent and sensible heat get transported away from the surface through turbulent mixing. Due to the tall, emergent canopy structures at the wetland sites, we see G_{aero} almost twice that at the alfalfa site, which has a short, smooth, regular canopy. In the windy Delta landscape, with strong westerly gusts from the Pacific Ocean, G_{aero} promotes turbulent fluxes, even at night (Figure 5b). Because G_{aero} is instrumental in transferring both latent and sensible heat to the atmosphere, the site's water availability is an important determinant of the relative partitioning of heat.

Alfalfa and the old wetland, with no exposed surface water, exhibit a regular diel cycle of G_{sfc} (Figure 5a). A thick layer of dead litter and a closed, mature canopy at the old wetland decouples the atmosphere from the underlying water, eliminating daytime storage of net radiation in the water column (Figure 4b). This is reflected in old wetland water temperatures that are 15–25% cooler than the water temperatures at the other wetland sites (Eichelmann et al., 2018). Without daytime storage, enhanced radiation at the old wetland is dissipated as latent and sensible heat flux during the day, when stomata are open (Figures 4c and 4d), by high G_{aero} (Figure 5b). In this way, the old wetland acts less as a flooded system, and more as a crop, with net radiation converted into daytime turbulent heat fluxes that result in a modest cooling effect compared to alfalfa.

These findings support work by Eichelmann et al. (2018), who found significant evapotranspiration differences between the more heterogeneous footprints of the young and intermediate wetlands and the closed-canopy old wetland, especially at night. The G_{sfc} measurements presented here support the finding that with closed, dense, wetland canopies, even when water is present underneath, evapotranspiration is largely mediated through daytime stomatal transpiration with minimal contribution of free evaporation. In juxtaposition, heightened nighttime G_{sfc} values at the more open young and intermediate wetlands, combined with ample energy storage in the water column, drive nighttime evaporation as latent energy—an important component of the energy balance for heterogeneous wetlands. Ongoing work to partition evaporation and transpiration in this system would provide a means to confirm these dynamics.

Impacts of the three critical biophysical properties that are affected by land use change—albedo, G_{sfc}, and G_{aero}—have been shown to counteract each other. Often, in a transition from field to forest, lowered albedo causes warming, while increased evaporative efficiency and G_{aero} cause cooling (Davin & de Noblet-Ducoudre, 2010; Juang et al., 2007). The integrated balance of these effects over a year determines the net biophysical impact of land use change. In the Delta system, radiative biophysical mechanisms alone cannot explain the observed temperature differences—the wetlands consistently exhibited lower albedo as compared to alfalfa (Table 1). The nonradiative mechanisms driving the observed daytime cooling effect in the Delta—through changes to G_{sfc}, G_{aero}, and storage—are essential to understanding the energy dynamics in this system.

Despite a warming effect of wetland cover during some spring and autumn months, the integrated biophysical impacts of restoration can provide significant daytime surface cooling depending on structural features, such as the ratio of open water to vegetation and the coupling of the water surface with the atmosphere. These complex factors are missing from many assessments of climatic impact of land use change (Myhre et al., 2013) but may govern critical feedbacks to plant physiology and boundary layer processes, especially in scenarios of large-scale land conversion (Burakowski et al., 2017; Gerken et al., 2018). This result emphasizes the importance of diagnosing and modeling specific biophysical changes likely to take place in novel land use transitions, like reflooding drained agricultural peatlands.

4.2. Implications for Vegetation and Boundary Layer Feedbacks

To understand the interaction of daytime T_{aero} reduction on productivity and plant physiology, we used a nonparametric binning approach to extract a response function from the 3-year data set. The alfalfa site experienced higher T_{aero}, especially compared to the young and intermediate wetland sites. Its net ecosystem productivity (NEP) also responded most negatively to rising T_{aero} (Figure 6a), even after removing the 5 days directly after harvest, when NEP is drastically reduced. The flooded wetland sites have more modulated responses to T_{aero}, each with an optimal between 25 °C and 30 °C, at which NEP is greatest (Figures 6b–6d). This is a slightly higher optimal T_{aero} than that recorded through isotopic cellulose measurements in trees covering a broad range of latitudes (Helliker & Richter, 2008). At higher than optimal T_{aero} in the wetland sites, NEP plateaus without dramatic declines, as we see at Alfalfa.

The effect of climatic warming on wetlands, and especially freshwater restored wetlands, is not well understood. Differential responses of plant communities may mediate energy, carbon, and nutrient budgets (Weltzin et al., 2000), although other work has documented state changes associated with warming across salt marsh-mangrove gradients (Feher et al., 2017), and increases in biomass in response to ambient warming (Baldwin et al., 2014). Surface temperature and energy balance changes could affect thermal hydrodynamic convection, an important driver of diffusive CH_4 emission (Poindexter et al., 2016), as well as plant-mediated

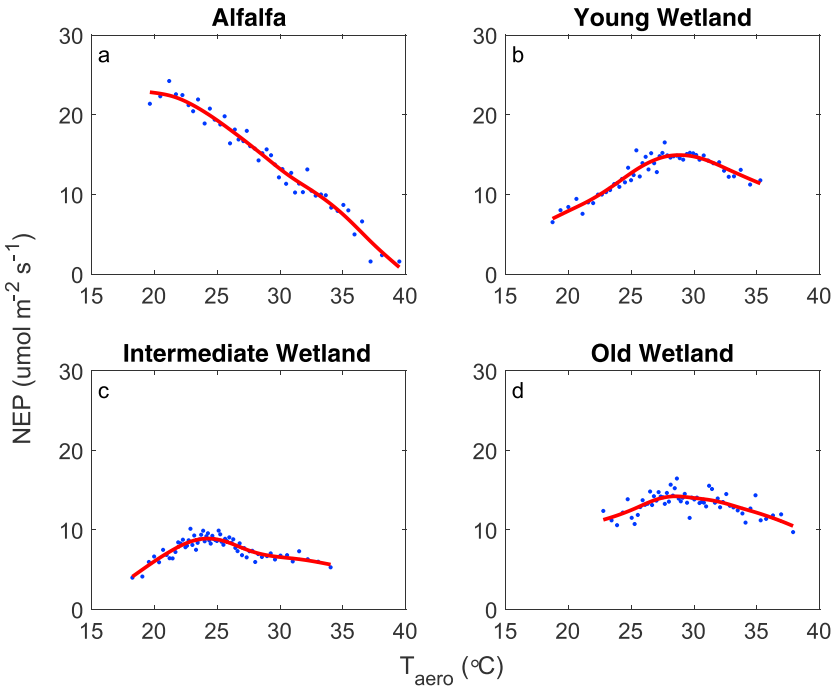

Figure 6. Daytime aerodynamic temperature bins (n = 50) as a function of net ecosystem productivity (NEP). Excluded 5 days after harvest at alfalfa site. Data are filtered for incoming photosynthetically active radiation (>1,500 μmol m^{-2} s^{-1}).

transfer of CH_4, which accounts for the majority of peatland CH_4 emissions (Dean et al., 2018). With California's climate projected to become warmer and drier into the future (Ficklin & Novick, 2017), wetland-induced surface cooling could be important in ameliorating physiological stress associated with high ambient air temperature and VPD, and potentially feedback to plant-mediated biogeochemical cycling.

Surface modulation by the wetlands could produce feedbacks on the PBL as entrainment from above and modifications to the PBL depth and atmospheric volume influence daily evolution of T_{air} in the mixed layer. Model computations, compared to tower-measured T_{air}, avoid confounding effects of temperature sensor calibration offsets, variable measurement height, and horizontal advection of heat. We used a simple EB-PBL model to understand the potential local atmospheric feedbacks to the surface properties at each of the study sites (Baldocchi & Ma, 2013). The model was run for cloudless growing season conditions, driven by measured diel VPD and incoming radiation (Rg_{in}), $S_{residual}$, and half-hourly values of G_{aero} and G_{sfc} computed from flux data (Figure S5).

The modeled T_{aero} closely matches the daytime dynamics of T_{aero}, with the young and intermediate wetlands much cooler, and the old wetland slightly cooler, than the alfalfa site (Figure 7a). The young and intermediate wetlands, with open water surfaces and relatively high G_{sfc} and G_{aero} throughout the day, resulted in lower T_{air} (Figure 7b) in the mixed layer by close to 5 °C. This is consistent with the findings of Helbig et al. (2016) who also found a PBL cooling effect due to wetland expansion, primarily for reasons related to enhanced latent heat and diminished sensible heat flux. With suppressed sensible heat flux, heterogeneous restored wetlands may also result in a lower boundary layer.

In other systems, with much less available moisture, enhanced G_{aero} could cause a mixed layer air temperature warming effect. In a nearby Mediterranean grassland and savannah system, the taller and rougher oak woodland caused a potential air temperature warming effect of 0.5 °C (Baldocchi & Ma, 2013). Our results suggest that surface property differences inherent in transitions from drained agricultural peatland land uses to restored wetlands could have significant cooling impacts on local climate, especially under situations of widespread restoration. This cooling effect is dependent on wetland canopy structure, however. The old wetland's surface properties promoted higher boundary layers and T_{air} slightly warmer than that over alfalfa by midday.

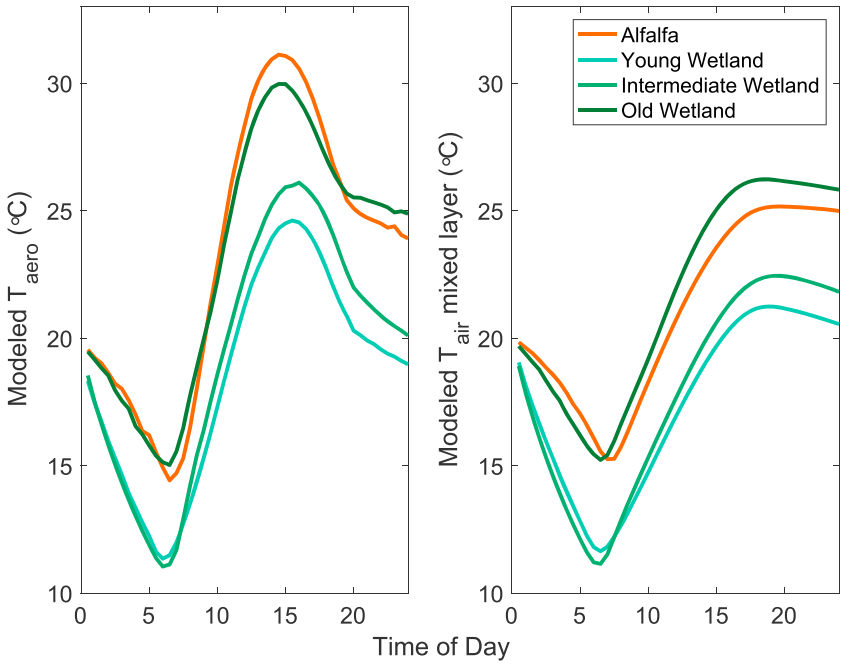

Figure 7. Modeled (a) aerodynamic surface temperature and (b) mixed layer air temperature, given the surface properties at each of the study sites (Figure S5), for a clear-sky growing season day.

4.3. Policy Implications and Future Work

Consideration of the biophysical impacts is critical to understanding how land use related policies and incentives will affect physiology and local to regional climate. While this is beginning to be recognized in forest land use transitions, other land use activities are being incentivized through methodologies as part of nascent climate change policies without a complete understanding of the biophysical impacts that could result. We hypothesized that the transition from drained agricultural peatlands planted with short-statured perennial alfalfa to managed wetlands with tall, emergent canopies is, in some ways, analogous to the biophysical impact of afforestation. In our analysis, the young and intermediate wetlands both exhibit cooler daytime and warmer nighttime surface conditions (Figure 3). Local tower-based air temperature measurements show a sizable (1.4–4.0 °C) reduction in diurnal temperature range at the young and intermediate wetland sites (Figure S4), which is similarly reported as an impact of reforestation (Alkama & Cescatti, 2016; Burakowski et al., 2017; Lee et al., 2011; Lejeune et al., 2018).

Transition from a short-statured, smooth alfalfa crop to a tall, emergent, heterogeneous wetland has the potential to enhance biogeochemical benefits of wetland restoration (Knox et al., 2015) by causing a daytime surface cooling effect, counteracting the ongoing and predicted increases in temperature associated with global climate change. Wetland transition from other dominant Delta crops may have different, possibly more enhanced, cooling effects. When designing climate mitigation projects, ecosystem structure and time since restoration must be more explicitly considered. Older wetlands tend to accrue a dense mat of dead litter after multiple seasons of blowdowns and storm damage (Schile et al., 2013), which have been shown to decouple the canopy air space from the water below (Goulden et al., 2007), effectively turning a mature wetland into a well-watered crop (Eichelmann et al., 2018). Restored wetland designs that feature tracts of open water that will not rapidly fill in with vegetation may promote this cooling effect, which otherwise could be diminished as maturing wetlands fill in with vegetation and create a closed canopy structure. Future work should more explicitly quantify the storage term in restored wetlands with dynamic and varied bathymetry.

In addition to wetland design, wetland extent and scale will play an important role in the degree of local to regional cooling. Results from a wetlands-adjacent rice field in the Delta show that increasing the size of flooded land cover from ~1 to ~5 km^2 between 2009 and 2014 caused a decrease in evapotranspiration

due to a decreasing oasis effect (Baldocchi et al., 2016). Where a mosaic of flooded patches in a semiarid climate will promote entrainment of warm dry air from above the PBL (the "oasis" effect) and enhance evaporation, larger tracts of flooded land could mitigate this feedback. Our study was performed during a time of relatively stable flooded land cover extent on the islands of interest, but future work should focus on modeling how much area and what kinds of orientations of flooded land cover will cause a meaningful effect across local to regional jurisdictions (Gerken et al., 2018).

These results are likely specific to restored, managed wetlands—with managed water tables and little current or outflow. Complete restoration to a more natural, tidal-influenced, and seasonally flood-influenced wetland is unlikely in California's highly managed water delivery system, especially given the policy goal to inhibit respiration and sequester carbon through permanent flooding. Connectivity with the preindustrial, natural watershed would have hydrological impacts that we cannot adequately address here (Mitsch et al., 2005). Designing and managing restored wetlands to provide a cooling effect could increase water use (Eichelmann et al., 2018), conflicting with important urban, agricultural, and habitat water demand in a semiarid California landscape characterized by large interannual variability in precipitation. This water cost must be considered in light of the integrated biophysical, biogeochemical, habitat, and levee stability benefits that are all associated with wetland restoration.

5. Conclusions

While biogeochemical impacts of land use change are most often considered, our results emphasize the need to include an assessment of biophysical impacts to fully understand how a land use change, such as wetland restoration, affects the albedo, water availability, roughness, and ultimately the T_{aero} of an ecosystem. Using 12 site years of eddy covariance data across a network of restored wetland and agricultural sites in the Sacramento-San Joaquin Delta, we show significant T_{aero} differences between restored wetlands and a dominant drained agricultural land use.

Heterogeneous wetlands with open water surfaces are characterized by increased daytime storage of energy, with reduced sensible heat during the day and enhanced latent heat during the night promoted by heightened G_{sfc} and G_{aero}, compared to the alfalfa land cover. This daytime cooling effect, of up to 2.1 °C to 5.1 °C, could be important in ameliorating the physiological stress of increasing temperature associated with climate change at the local scale. Using a simple EB-PBL model, we show that the surface and aerodynamic properties that result in wetland T_{aero} cooling at the young and intermediate wetlands also cause a reduction in mixed layer T_{air}. Future studies should explore the potential teleconnection between large-scale wetland restoration and climate over broader regional scales. Along with habitat creation and levee stabilization, the biophysical surface cooling effects of restored wetlands could enhance the biogeochemical sequestration benefits.

While this study was limited to the biophysical impacts of restored, managed wetlands under the scenario in which they are converted from a perennial field crop, future studies could expand this analysis to other crops and natural wetland systems. Despite the challenges with reconciling radiative and nonradiative impacts of land use change, especially in complex ecosystems such as wetlands, it is critical to understand the biophysical processes that will be affected under proposed land use change scenarios. With a renewed focus on the importance of natural and working lands in climate change mitigation, we must ensure that land use changes incentivized for their biogeochemical benefit do not have unforeseen negative consequences.

Acknowledgments
Data for the four study sites are available through Ameriflux at https://ameriflux.lbl.gov. Citations can be found in the references. This work was supported by the California Department of Water Resources (DWR), through a contract from the California Department of Fish and Wildlife, and the United States Department of Agriculture (NIFA grant 2011-67003-30371). Funding for the AmeriFlux core sites was provided by the U.S. Department of Energy's Office of Science (AmeriFlux contract 7079856). K. S. H. was supported by the California Sea Grant Delta Science Fellowship. This material is based upon work supported by the Delta Stewardship Council Delta Science Program under grant 2271 and California Sea Grant College Program Project R/SF-70. The contents of this material do not necessarily reflect the views and policies of the Delta Stewardship Council or California Sea Grant nor does mention of trade names or commercial products constitute endorsement or recommendation for use. The authors would like to thank the farmers for their cooperation during the project, as well as Bryan Brock from the DWR for his support and management of the wetlands.

References

Alkama, R., & Cescatti, A. (2016). Biophysical climate impacts of recent changes in global forest cover. *Science*, *351*(6273), 600–604. https://doi.org/10.1126/science.aac8083

Anderson, R. G., Canadell, J. G., Randerson, J. T., Jackson, R. B., Hungate, B. A., Baldocchi, D. D., et al. (2011). Biophysical considerations in forestry for climate protection. *Frontiers in Ecology and the Environment*, *9*(3), 174–182. https://doi.org/10.1890/090179

Arneth, A., Harrison, S. P., Zaehle, S., Tsigaridis, K., Menon, S., Bartlein, P. J., et al. (2010). Terrestrial biogeochemical feedbacks in the climate system. *Nature Geoscience*, *3*(8), 525–532. https://doi.org/10.1038/ngeo905

Atwater, B. F., Conard, S. G., Dowden, J. N., Hedel, C. W., MacDonald, R. L., & Savage, W. (1979). History, landforms, and vegetation of the estuary's tidal marshes. In T. J. Conomos (Ed.), *San Francisco Bay: the urbanized estuary* (pp. 347–385). San Francisco, CA: AAAS Pacific Division.

Baldocchi, D. D. (2018a). Ameriflux US-Tw3 Twitchell Alfalfa. https://doi.org/10.17190/AMF/1246149

Baldocchi, D. D. (2018b). Ameriflux US-Tw4 Twitchell East End Wetland. https://doi.org/10.17190/AMF/1246151

Baldocchi, D. D. (2018c). Ameriflux US-Myb Mayberry Wetland. https://doi.org/10.17190/AMF/1246139

Baldocchi, D. D. (2018d). Ameriflux US-Tw1 Twitchell Wetland West Pond. https://doi.org/10.17190/AMF/1246147
Baldocchi, D. D., Hicks, B. B., & Meyers, T. P. (1988). Measuring biosphere-atmosphere exchanges of biologically related gases with micrometeorological methods. *Ecology*, *69*, 1331–1340.
Baldocchi, D. D., Knox, S. H., Dronova, I., Verfaillie, J., Oikawa, P., Sturtevant, C., et al. (2016). The impact of expanding flooded land area on the annual evaporation of rice. *Agricultural and Forest Meteorology*, *223*, 181–193. https://doi.org/10.1016/j.agrformet.2016.04.001
Baldocchi, D. D., & Ma, S. (2013). How will land use affect air temperature in the surface boundary layer? Lessons learned from a comparative study on the energy balance of an oak savanna and annual grassland in California, USA. *Tellus B*, *65*(1). https://doi.org/10.3402/tellusb.v65i0.19994
Baldwin, A. H., Jensen, K., & Schonfeldt, M. (2014). Warming increases plant biomass and reduces diversity across continents, latitudes, and species migration scenarios in experimental wetland communities. *Global Change Biology*, *20*(3), 835–850. https://doi.org/10.1111/gcb.12378
Barr, A. G., & Betts, A. K. (1997). Radiosonde boundary layer budgets above a boreal forest. *Journal of Geophysical Research*, *102*, 29,205–29,212. https://doi.org/10.1029/97JD01105
Barr, J. G., Engel, V., Fuentes, J. D., Fuller, D. O., & Kwon, H. (2013). Modeling light use efficiency in a subtropical mangrove forest equipped with CO_2 eddy covariance. *Biogeosciences*, *10*(3), 2145–2158. https://doi.org/10.5194/bg-10-2145-2013
Bianco, L., Djalalova, I. V., King, C. W., & Wilczak, J. M. (2011). Diurnal evolution and annual variability of boundary-layer height and its correlation to other meteorological variables in California's Central Valley. *Boundary-Layer Meteorology*, *140*(3), 491–511. https://doi.org/10.1007/s10546-011-9622-4
Bonan, G. B. (2008). Forests and climate change: Forcings, feedbacks, and the climate benefits of forests. *Science*, *320*(5882), 1444–1449. https://doi.org/10.1126/science.1155121
Bonfils, C., Duffy, P. B., Santer, B. D., Wigley, T. M. L., Lobell, D. B., Phillips, T. J., & Doutriaux, C. (2007). Identification of external influences on temperatures in California. *Climatic Change*, *87*, 43–55.
Bridgham, S. D., Cadillo-Quiroz, H., Keller, J. K., & Zhuang, Q. (2013). Methane emissions from wetlands: Biogeochemical, microbial, and modeling perspectives from local to global scales. *Global Change Biology*, *19*(5), 1325–1346. https://doi.org/10.1111/gcb.12131
Bright, R. M., Davin, E., O'Halloran, T., Pongratz, J., Zhao, K., & Cescatti, A. (2017). Local temperature response to land cover and management change driven by non-radiative processes. *Nature Climate Change*, *7*(4), 296–302. https://doi.org/10.1038/nclimate3250
Brovkin, V., Ganopolski, A., Claussen, M., Kubatzki, C., & Petoukhov, V. (1999). Modelling climate response to historical land cover change. *Global Ecology and Biogeography*, *8*(6), 509–517. https://doi.org/10.1046/j.1365-2699.1999.00169.x
Burakowski, E., Tawfik, A., Ouimette, A., Lepine, L., Novick, K., Ollinger, S., et al. (2017). The role of surface roughness, albedo, and Bowen ratio on ecosystem energy balance in the Eastern United States. *Agricultural and Forest Meteorology*, *249*, 367–376.
Cescatti, A., Marcolla, B., Santhana Vannan, S. K., Pan, J. Y., Román, M. O., Yang, X., et al. (2012). Intercomparison of MODIS albedo retrievals and in situ measurements across the global FLUXNET network. *Remote Sensing of Environment*, *121*, 323–334. https://doi.org/10.1016/j.rse.2012.02.019
Davin, E. L., & de Noblet-Ducoudre, N. (2010). Climatic impact of global-scale deforestation: Radiative versus nonradiative processes. *Journal of Climate*, *23*(1), 97–112. https://doi.org/10.1175/2009JCLI3102.1
Dean, J. F., Middelburg, J. J., Röckmann, T., Aerts, R., Blauw, L. G., Egger, M., et al. (2018). Methane feedbacks to the global climate system in a warmer world. *Reviews of Geophysics*, *56*, 207–250. https://doi.org/10.1002/2017RG000559
Detto, M., Baldocchi, D., & Katul, G. G. (2010). Scaling properties of biologically active scalar concentration fluctuations in the atmospheric surface layer over a managed peatland. *Boundary-Layer Meteorology*, *136*(3), 407–430. https://doi.org/10.1007/s10546-010-9514-z
Deverel, S. J., Ingrum, T., & Leighton, D. (2016). Present-day oxidative subsidence of organic soils and mitigation in the Sacramento-San Joaquin Delta, California, USA. *Hydrogeology Journal*, *24*(3), 569–586. https://doi.org/10.1007/s10040-016-1391-1
D'Odorico, P., Fuentes, J. D., Pockman, W. T., Collins, S. L., He, Y., Medeiros, J. S., et al. (2010). Positive feedback between microclimate and shrub encroachment in the northern Chihuahuan desert. *Ecosphere*, *1*, art17.
Drexler, J. Z., Fontaine, C. S., & Deverel, S. J. (2009). The legacy of wetland drainage on the remaining peat in the Sacramento-San Joaquin Delta, California, USA. *Wetlands*, *29*(1), 372–386. https://doi.org/10.1672/08-97.1
Eichelmann, E., Hemes, K. S., Knox, S. H., Oikawa, P. Y., Chamberlain, S. D., Sturtevant, C., et al. (2018). The effect of land cover type and structure on evapotranspiration from agricultural and wetland sites in the Sacramento–San Joaquin River Delta, California. *Agricultural and Forest Meteorology*, *256-257*, 179–195. https://doi.org/10.1016/j.agrformet.2018.03.007
Falge, E., Baldocchi, D., Olson, R., Anthoni, P., Aubinet, M., Bernhofer, C., et al. (2001). Short communication: Gap filling strategies for long term energy flux data sets. *Agricultural and Forest Meteorology*, *107*(1), 71–77. https://doi.org/10.1016/S0168-1923(00)00235-5
Feher, L. C., Osland, M. J., Griffith, K. T., Grace, J. B., Howard, R. J., Stagg, C. L., et al. (2017). Linear and nonlinear effects of temperature and precipitation on ecosystem properties in tidal saline wetlands. *Ecosphere*, *8*(10). https://doi.org/10.1002/ecs2.1956
Ficklin, D. L., & Novick, K. A. (2017). Historic and projected changes in vapor pressure deficit suggest a continental-scale drying of the United States atmosphere. *Journal of Geophysical Research: Atmospheres*, *122*, 2061–2079. https://doi.org/10.1002/2016JD025855
Georgescu, M., Lobell, D. B., & Field, C. B. (2011). Direct climate effects of perennial bioenergy crops in the United States. *Proceedings of the National Academy of Sciences of the United States of America*, *108*(11), 4307–4312. https://doi.org/10.1073/pnas.1008779108
Gerken, T., Bromley, G. T., & Stoy, P. C. (2018). Surface moistening trends in the northern North American Great Plains increase the likelihood of convective initiation. *Journal of Hydrometeorology*, *19*(1), 227–244. https://doi.org/10.1175/JHM-D-17-0117.1
Goulden, M. L., Litvak, M., & Miller, S. D. (2007). Factors that control Typha marsh evapotranspiration. *Aquatic Botany*, *86*(2), 97–106. https://doi.org/10.1016/j.aquabot.2006.09.005
Griscom, B. W., Adams, J., Ellis, P. W., Houghton, R. A., Lomax, G., Miteva, D. A., et al. (2017). Natural climate solutions. *Proceedings of the National Academy of Sciences of the United States of America*, *114*(44), 11,645–11,650.
Hanson, B., Putnam, D., & Snyder, R. (2007). Deficit irrigation of alfalfa as a strategy for providing water for water-short areas. *Agricultural Water Management*, *93*(1-2), 73–80. https://doi.org/10.1016/j.agwat.2007.06.009
Hatala, J. A., Detto, M., Sonnentag, O., Deverel, S. J., Verfaillie, J., & Baldocchi, D. D. (2012). Greenhouse gas (CO_2, CH_4, $H2_O$) fluxes from drained and flooded agricultural peatlands in the Sacramento-San Joaquin Delta. *Agriculture, Ecosystems & Environment*, *150*, 1–18. https://doi.org/10.1016/j.agee.2012.01.009
He, Y., D'Odorico, P., & De Wekker, S. F. J. (2015). The role of vegetation-microclimate feedback in promoting shrub encroachment in the northern Chihuahuan desert. *Global Change Biology*, *21*(6), 2141–2154. https://doi.org/10.1111/gcb.12856
Helbig, M., Wischnewski, K., Kljun, N., Chasmer, L., Quinton, W. L., Detto, M., & Sonnentag, O. (2016). Regional atmospheric cooling and wetting effect of permafrost thaw-induced boreal forest loss. *Global Change Biology*, *22*, 4048–4066.

Helliker, B. R., & Richter, S. L. (2008). Subtropical to boreal convergence of tree-leaf temperatures. *Nature*, *454*(7203), 511–514. https://doi.org/10.1038/nature07031

Hemes, K. S., Chamberlain, S. D., Eichelmann, E., Knox, S. H., & Baldocchi, D. D. (2018). A biogeochemical compromise: The high methane cost of sequestering carbon in restored wetlands. *Geophysical ResearchLetters*, *45*. https://doi.org/10.1029/2018GL077747

Humphreys, E. R., Lafleur, P. M., Flanagan, L. B., Hedstrom, N., Syed, K. H., Glenn, A. J., & Granger, R. (2006). Summer carbon dioxide and water vapor fluxes across a range of northern peatlands. *Journal of Geophysical Research*, *111*, G04011. https://doi.org/10.1029/2005JG000111

Jackson, R. B., Randerson, J. T., Canadell, J. G., Anderson, R. G., Avissar, R., Baldocchi, D. D., et al. (2008). Protecting climate with forests. *Environmental Research Letters*, *3*(4), 044006. https://doi.org/10.1088/1748-9326/3/4/044006

Jarvis, P., & McNaughton, K. G. (1986). Stomatal control of transpiration: Scaling up from leaf to region. *Advances in Ecological Research*, *15*, 1–49. https://doi.org/10.1016/S0065-2504(08)60119-1

Juang, J. Y., Katul, G., Siqueira, M., Stoy, P., & Novick, K. (2007). Separating the effects of albedo from eco-physiological changes on surface temperature along a successional chronosequence in the southeastern United States. *Geophysical Research Letters*, *34*, L21408. https://doi.org/10.1029/2007GL031296

Kaimal, J. C., Wyngaard, J. C., Izumi, Y., & Coté, O. R. (1972). Spectral characteristics of surface-layer turbulence. *Quarterly Journal of the Royal Meteorological Society*, *98*(417), 563–589. https://doi.org/10.1002/qj.49709841707

Knauer, J., Zaehle, S., Medlyn, B. E., Reichstein, M., Williams, C. A., Migliavacca, M., et al. (2017). Towards physiologically meaningful water-use efficiency estimates from eddy covariance data. *Global Change Biology*, *24*, 694–710.

Knox, S. H., Matthes, J. H., Sturtevant, C., Oikawa, P. Y., Verfaillie, J., & Baldocchi, D. (2016). Biophysical controls on interannual variability in ecosystem scale CO_2 and CH_4 exchange in a California rice paddy. *Journal of Geophysical Research: Biogeosciences*, *121*, 978–1001. https://doi.org/10.1002/2015JG003247

Knox, S. H., Sturtevant, C., Matthes, J. H., Koteen, L., Verfaillie, J., & Baldocchi, D. (2015). Agricultural peatland restoration: Effects of land-use change on greenhouse gas (CO_2 and CH_4) fluxes in the Sacramento-San Joaquin Delta. *Global Change Biology*, *21*(2), 750–765. https://doi.org/10.1111/gcb.12745

Lee, X., Goulden, M. L., Hollinger, D. Y., Barr, A., Black, T. A., Bohrer, G., et al. (2011). Observed increase in local cooling effect of deforestation at higher latitudes. *Nature*, *479*(7373), 384–387. https://doi.org/10.1038/nature10588

Lejeune, Q., Davin, E. L., Gudmundsson, L., Winckler, J., & Seneviratne, S. I. (2018). Historical deforestation locally increased the intensity of hot days in northern mid-latitudes. *Nature Climate Change*, *8*(5), 386–390. https://doi.org/10.1038/s41558-018-0131-z

Lobell, D. B., Bala, G., & Duffy, P. B. (2006). Biogeophysical impacts of cropland management changes on climate. *Geophysical Research Letters*, *33*, L06708. https://doi.org/10.1029/2005GL025492

Lobell, D. B., & Bonfils, C. (2008). The effect of irrigation on regional temperatures: A spatial and temporal analysis of trends in California, 1934-2002. *Journal of Climate*, *21*(10), 2063–2071. https://doi.org/10.1175/2007JCLI1755.1

Luyssaert, S., Jammet, M., Stoy, P. C., Estel, S., Pongratz, J., Ceschia, E., et al. (2014). Land management and land-cover change have impacts of similar magnitude on surface temperature. *Nature Climate Change*, *4*(5), 389–393. https://doi.org/10.1038/nclimate2196

Ma, S., Osuna, J. L., Verfaillie, J., & Baldocchi, D. D. (2017). Photosynthetic responses to temperature across leaf–canopy–ecosystem scales: A 15-year study in a Californian oak-grass savanna. *Photosynthesis Research*, *0*, 1–15.

Mahmood, R., Pielke, R. A. Sr., Hubbard, K. G., Niyogi, D., Dirmeyer, P. A., McAlpine, C., et al. (2014). Land cover changes and their biogeophysical effects on climate. *International Journal of Climatology*, *34*(4), 929–953. https://doi.org/10.1002/joc.3736

Mcalpine, C. A., Ryan, J. G., Seabrook, L., Thomas, S., Dargusch, P. J., Syktus, J. I., et al. (2010). More than CO 2: A broader paradigm for managing climate change and variability to avoid ecosystem collapse. *Current Opinion in Environmental Sustainability*, *2*, 334–346.

McNaughton, K. G., & Spriggs, T. W. (1986). A mixed-layer model for regional evaporation. *Boundary-Layer Meteorology*, *34*(3), 243–262. https://doi.org/10.1007/BF00122381

Medellín-Azuara, J., Kyaw Tha Paw U., Yufang Jin, Quinn Hart, Eric Kent, Jenae Clay, et al. (2016). Estimation of Crop Evapotranspiration in the Sacramento San Joaquin Delta for the 2014–2015 Water Year, Interim Report.

Miller, R. L., Fram, M., Fujii, R., & Wheeler, G. (2008). Subsidence reversal in a re-established wetland in the Sacramento-San Joaquin Delta, California, USA. *San Francisco Estuary and Watershed Science*, *6*(3). https://doi.org/10.15447/sfews.2008v6iss3art1

Mitsch, W. J., Zhang, L., Anderson, C. J., Altor, A. E., & Hernández, M. E. (2005). Creating riverine wetlands: Ecological succession, nutrient retention, and pulsing effects. *Ecological Engineering*, *25*(5), 510–527. https://doi.org/10.1016/j.ecoleng.2005.04.014

Moffat, A. M., Papale, D., Reichstein, M., Hollinger, D. Y., Richardson, A. D., Barr, A. G., et al. (2007). Comprehensive comparison of gap-filling techniques for eddy covariance net carbon fluxes. *Agricultural and Forest Meteorology*, *147*(3-4), 209–232. https://doi.org/10.1016/j.agrformet.2007.08.011

Monteith, J. L. (1965). Evaporation and environment. *Symposia of the Society for Experimental Biology*, *19*, 205–234.

Monteith, J. L. (1981). Evaporation and surface temperature. *Quarterly Journal of the Royal Meteorological Society*, *107*(451), 1–27. https://doi.org/10.1002/qj.49710745102

Mount, J., & Twiss, R. (2005). Subsidence, sea level rise, and seismicity in the Sacramento–San Joaquin Delta. *San Francisco Estuary & Watershed Science*, *3*(1). https://doi.org/10.15447/sfews.2005v3iss1art7

Myhre, G., Shindell, D., Bréon, F.-M., Collins, W., Fuglestvedt, J., Huang, J., et al. (2013). 2013: Anthropogenic and natural radiative forcing. In T. F. Stocker, et al. (Eds.), *Climate change 2013: The physical science basis. Contribution of working group I to the fifth assessment report of the intergovernmental panel on climate change* (Chap. 8, pp. 659–740). Cambridge, UK and New York: Cambridge University Press.

Papale, D., Reichstein, M., Aubinet, M., Canfora, E., Bernhofer, C., Kutsch, W., et al. (2006). Towards a standardized processing of net ecosystem exchange measured with eddy covariance technique: Algorithms and uncertainty estimation. *Biogeosciences*, *3*(4), 571–583. https://doi.org/10.5194/bg-3-571-2006

Paustian, K., Lehmann, J., Ogle, S., Reay, D., Robertson, G. P., & Smith, P. (2016). Climate-smart soils. *Nature*, *532*(7597), 49–57. https://doi.org/10.1038/nature17174

PawU, K. T., & Gao, W. (1988). Applications of solutions to non-linear energy budget equations. *Agricultural and Forest Meteorology*, *43*(2), 121–145. https://doi.org/10.1016/0168-1923(88)90087-1

Perugini, L., Caporaso, L., Marconi, S., Cescatti, A., Quesada, B., de Noblet, N., et al. (2017). Biophysical effects on temperature and precipitation due to land cover change. *Environmental Research Letters*, *12*, 053002. https://doi.org/10.1088/1748-9326/aa6b3f

Petrescu, A. M. R., Lohila, A., Tuovinen, J. P., Baldocchi, D. D., Desai, A. R., Roulet, N. T., et al. (2015). The uncertain climate footprint of wetlands under human pressure. *Proceedings of the National Academy of Sciences of the United States of America*, *112*(15), 4594–4599. https://doi.org/10.1073/pnas.1416267112

Poindexter, C. M., Baldocchi, D. D., Matthes, J. H., Knox, S. H., & Variano, E. A. (2016). The contribution of an overlooked transport process to a wetland's methane emissions. *Geophysical Research Letters*, *43*, 6276–6284. https://doi.org/10.1002/2016GL068782

Raupach, M. R. (1998). Influences of local feedbacks on land-air exchanges of energy and carbon. *Global Change Biology*, *4*(5), 477–494. https://doi.org/10.1046/j.1365-2486.1998.t01-1-00155.x

Rotenberg, E., & Yakir, D. (2010). Contributions of semi-arid forests to the climate system. *Science*, *327*(5964), 451–454. https://doi.org/10.1126/science.1179998

Schile, L. M., Byrd, K. B., Windham-Myers, L., & Kelly, M. (2013). Accounting for non-photosynthetic vegetation in remote-sensing-based estimates of carbon flux in wetlands. *Remote Sensing Letters*, *4*(6), 542–551. https://doi.org/10.1080/2150704X.2013.766372

Stanhill, G. (1970). Some results of helicopter measurements of the albedo of different land surfaces. *Solar Energy*, *13*(1), 59–66. https://doi.org/10.1016/0038-092X(70)90007-1

Thom, A. S. (1972). Momentum, mass and heat exchange of vegetation. *Quarterly Journal of the Royal Meteorological Society*, *98*(415), 124–134. https://doi.org/10.1002/qj.49709841510

Tian, H., Lu, C., Ciais, P., Michalak, A. M., Canadell, J. G., Saikawa, E., et al. (2016). The terrestrial biosphere as a net source of greenhouse gases to the atmosphere. *Nature*, *531*(7593), 225–228. https://doi.org/10.1038/nature16946

Verma, S. B. (1989). Aerodynamic resistances to transfers of heat, mass and momentum. In T. A. Black, D. L. Spittlehouse, M. D. Novak & D. T. Price (Eds.), *Estimation of areal evapotranspiration* (pp. 13–20). Wallingford, Oxfordshire: International Association of Hydrological Sciences.

Webb, E. K., Pearman, G. I., & Leuning, R. (1980). Correction of flux measurements for density effects due to heat and water vapour transfer. *Quarterly Journal of the Royal Meteorological Society*, *106*(447), 85–100. https://doi.org/10.1002/qj.49710644707

Weir, W. W. (1950). Subsidence of Peatlands of the Sacramento-San Joaquin Delta, California. *Hilgardia*, *20*(3), 37–56. https://doi.org/10.3733/hilg.v20n03p037

Weltzin, J. F., Pastor, J., Harth, C., Bridgham, S. D., Updegraff, K., & Chapin, C. T. (2000). Response of bog and fen plant communities to warming and water-table manipulations. *Ecology*, *81*(12), 3464–3478. https://doi.org/10.1890/0012-9658(2000)081[3464:ROBAFP]2.0.CO;2

Wilson, K., Goldstein, A., Falge, E., Aubinet, M., Baldocchi, D., Berbigier, P., et al. (2002). Energy balance closure at FLUXNET sites. *Agricultural and Forest Meteorology*, *113*(1-4), 223–243. https://doi.org/10.1016/S0168-1923(02)00109-0

Zhao, K., & Jackson, R. B. (2014). Biophysical forcings of land-use changes from potential forestry activities in North America. *Ecological Monographs*, *84*(2), 329–353. https://doi.org/10.1890/12-1705.1